ISSN 0915-633X

NATIONAL INSTITUTE FOR FUSION SCIENCE

Formation and 'Self-Healing' of Magnetic Islands in Finite-β Helias Equilibria

T. Hayashi, T. Sato, P. Merkel, J. Nührenberg and U. Schwenn

(Received – Jan. 6, 1994)

NIFS-269 Jan. 1994

RESEARCH REPORT
NIFS Series

NAGOYA, JAPAN

FORMATION AND 'SELF-HEALING' OF MAGNETIC ISLANDS IN FINITE-β HELIAS EQUILIBRIA

T.HAYASHI, T.SATO

National Institute for Fusion Science, Furocho, Nagoya, Japan

P.MERKEL, J.NÜHRENBERG, U.SCHWENN

Max-Planck-Institut für Plasmaphysik

IPP-EURATOM Association

D-8046 Garching bei München

Federal Republic of Germany

ABSTRACT

The behaviour of finite-pressure-induced magnetic islands is numerically analyzed for three-dimensional magnetohydrodynamic equilibria of the Helias configuration by using a three-dimensional equilibrium code. It is found that an island chain is generated on the 5/6 rational surface, when such a surface appears in the plasma region of the finite-β equilibrium. The island chain, however, is not so dangerous as to destroy the plasma confinement even if it appears in a vanishingly small shear region. Thus, a high β equilibrium with clear magnetic surfaces can be realized. Moreover, it is definitely confirmed that the finite pressure effect sometimes exhibits an unexpectedly good aspect, namely, that the vacuum islands are removed as β increases, which can be called 'self-healing' of islands. This property can be explained by the numerically discovered fact that the phases of islands induced by the finite-pressure effect are always locked in the same phase regardless of β.

keywords; helical system, Helias, 3-D MHD equilibrium, magnetic surface breaking, finite pressure effect, equilibrium beta limit, self-healing, magnetic island, Wendelstein 7-X

I. INTRODUCTION

In order to answer the indeterminate question[1–5] of whether or not a three-dimensional (3D) magnetohydrodynamic finite-β equilibrium can keep clearly nested magnetic surfaces, the 3D equilibrium code HINT was developed,[6] which does not a priori demand the existence of regularly nested magnetic surfaces. In previous papers,[7–9] we numerically analyzed the island formation for the $l = 2$ heliotron/torsatron configuration by using this code. One important discovery obtained was that magnetic surfaces are broken by the finite pressure effect in an actual helical configuration, and the breaking often imposes severer limitation on the equilibrium β than the Shafranov shift. It was also found that various physical parameters, such as the aspect ratio of the configuration and the magnitude of the external poloidal fields, can give significant influences on the occurrence of the breaking as β increases. In this paper, we study properties of magnetic islands induced by the finite pressure effect for the equilibrium of a non-axisymmetric toroidal configuration, Helias.[10]

Although both Helias and heliotron/torsatron are categorized as stellarator configurations, they are quite different in many aspects. While the $l = 2$ heliotron/torsatron is characterized as a medium to high shear configuration, Helias is classified as a low shear configuration. Consequently, the number of relevant dangerous rational surfaces is smaller for Helias, but a small resonant field, if any, can produce a large island. Another noticeable characteristic for Helias is that the amount of the Pfirsch-Schlüter current, which is the main origin of the finite-pressure-driven islands, is significantly reduced as an integral characteristic of this configuration. Thus, the way of island formation as a function of β for Helias is significantly different from the way for heliotron/torsatron.

The Wendelstein 7-X (W7-X) device has been designed as a next generation stellarator device.[11] Among a class of the Helias configurations, W7-X adopts a configuration with five field periods and with vanishing bootstrap current;[12] resistive as well as ideal MHD modes are avoided by magnetic-well stabilization throughout the plasma volume. In this paper, we analyze a magnetic configuration close to the one proposed for W7-X. The magnetic surfaces of the W7-X configuration can be designed such that the low-order rational surfaces, with rotational transform $\iota = 5/5$ and $5/6$, can be avoided. It is however of interest to study the finite-pressure behaviour of the 5/6 island chain to assess whether this should be dangerous or not. For this study, we choose a vacuum field situation in which at finite pressure this island chain occurs and resides at about half the plasma radius in a position of vanishing shear.

In the process of the equilibrium calculations for Helias described in this paper, we found

a remarkable property of magnetic islands induced by the finite pressure effect; the islands, in some cases, show a property of 'self-healing', i.e. they tend to shrink as β increases.

In this paper, in Sec. II, we discuss the formation of magnetic islands in a finite-β Helias equilibrium. In Sec. III, the evidence is shown that in some cases the 'self-healing' of islands can occur. Discussion and summary are given in Sec. IV. In the Appendix, we describe a slight modification of the geometry of the HINT code which has been made to treat the Helias configuration properly.

II. ISLAND FORMATION IN FINITE β HELIAS

Shown in Fig.1 are Poincaré plots of a vacuum field of Helias, which we analyze in this paper, for two poloidal cross sections, $\phi = 0$ and $\frac{\pi}{5}$, where ϕ is the toroidal angle. Those are called 'bean-shaped' and 'triangular' cross sections, respectively. In the HINT code, an equilibrium is calculated on grid points, which have rectangular calculation-boundary in a poloidal cross section (a grid box). The position of the grid box is also plotted in the figure. The vacuum field is calculated by using a current distribution on a surface which lies completely outside the grid box. A current-carrying surface fulfilling this condition is used, which was confirmed to produce approximately the same vacuum field as obtained from an optimized coil set that is proposed for W7-X; for example, the last closed surface lie just outside the five islands ($\iota = \frac{5}{5}$) for both vacuum fields.

The corresponding radial profiles of the rotational transform ι of the vacuum field, as well as of a finite-β field, are plotted in Fig.2. The rotational transform at the magnetic axis, ι_0, for the vacuum field is set slightly greater than $\frac{5}{6}$, a candidate for the most dangerous rational surface as for the island formation in the plasma core. The ι profile has almost vanishing shear in the inner part of the minor radius, but has a small shear in the outer part, in which ι increases monotonically toward the plasma boundary, up to slightly greater than 1.0 on the boundary for the vacuum field.

In equilibrium calculations in this paper, the pressure profile is given as $p = p_0(1 - \psi)^2$ (until islands appear), where ψ is the normalized toroidal flux. Equilibrium calculations are made on grids with the size of $73 \times 73 \times 41$ points for half a field period of the torus. Numerical validity of the equilibrium calculation is checked by comparing results obtained by using different sizes of grids ($49 \times 49 \times 29$) for the same configuration; there appears no significant difference in sizes as well as phases of island chains that are formed for each grid-

size calculations.[9] This result confirms that the observed formation of island chains, which we will discuss in the following, is not due to a numerical artifact.

One characteristic in the behaviour of ι profile is that ι_0 decreases as β increases, as is shown in Fig.2 (b); it may be interesting to note that in standard cases of $l = 2$ heliotron/torsatron configurations, ι_0 usually increases with β.[7] Because of this behaviour, the $\frac{5}{6}$ rational surface can come into the plasma region; first it appears near the magnetic axis, and moves outward as β increases. When β is low, no noticeable island appears even if the $\frac{5}{6}$ surface exists near the magnetic axis. However, the $\frac{5}{6}$ island chain is induced when the $\frac{5}{6}$ surface resides at about half the plasma radius, where the plasma β at the magnetic axis is $\beta_0 = 7.2\%$. The formation of the island can be observed in the ι profile as the flat area at $\iota = \frac{5}{6}$ in Fig.2 (b).

The radial profiles of the magnetic well $W(\bar{r})$ for the vacuum field and for the finite-β field are also plotted in Fig.2. Here, W is defined as $W(\bar{r}) \equiv \{(U(0) - U(\bar{r}))/U(0)\} \times 100(\%)$, where the specific volume $U = (1/N) \int_N (dl/B)$ is evaluated on a surface with average minor radius $\bar{r}$. The vacuum field has a magnetic well throughout the whole minor radius, since $dW/d\bar{r}$ is positive everywhere. The well is deepened as β increases.

The shape of the chain of $\frac{5}{6}$ island which appears in the finite-β equilibria ($\beta_0 = 7.2\%$) is visibly shown in Fig.3 by Poincaré plots of the magnetic field for two poloidal cross sections, $\phi = 0$ and $\frac{\pi}{5}$. The island chain appears in quite a low shear region. An important result, however, is that even this situation is not so serious as to destroy the plasma as is shown in this figure; most of the plasma region is covered by clearly nested surfaces. Corresponding to the formation of islands in the magnetic field structure as is shown in Fig.3, the island structure is also formed in the pressure profile, as is shown in Fig.4, where the pressure is flattened inside the $\frac{5}{6}$ island. We would like to note that in the HINT code the pressure is automatically calculated even inside islands as a result of the incorporated calculation step which makes the pressure uniform along each field line. Coincidence of magnetic and pressure islands, which is demonstrated explicitly here in computational stellarator equilibria for the first time, proves validity of the code.

In the boundary region, the $\frac{5}{5}$ island chain, which existed just inside the outermost surface in the vacuum field, lies in the ergodic region. Now, the last closed surface lies inside the $\frac{5}{5}$ islands and the islands are partially ergodized. However, the positions of the $\frac{5}{5}$ islands and of the boundary surfaces do not vary significantly. This is a consequence of the very small radial shift of free-boundary Helias equilibria, owing to the significantly reduced Pfirsch-Schlüter current in the configuration. This behaviour is an important condition for a successful divertor

operation in finite-β equilibria of the W7-X device.[13]

When β is further increased, the $\frac{5}{6}$ island chain comes to the boundary region. Although β is increased, the size of the island chain does not change so much. This may be due to the increased shear in the boundary region. Finally, the quality of magnetic surfaces is deteriorated when β_0 is increased beyond, say, 15%, because island chains with higher mode numbers grow on several higher-order rational surfaces simultaneously.

III. 'SELF-HEALING' OF MAGNETIC ISLANDS

So far we have analyzed finite-pressure effects on equilibria from the point of view of 'formation' of islands. Now, it may be interesting to investigate whether the opposite process, namely, 'self-healing' of islands, can occur or not.

Here we note the following indication given by computational experience. As for the islands induced due to the finite-pressure effect, the phase of the islands is independent of the value of β, and does not depend on the details of the way one increases β in equilibrium calculations; for the case discussed in the section II, the $\frac{5}{6}$ island chain always has the x-point at the outer side in the 'triangular' poloidal cross section ($\phi = \frac{\pi}{5}$), as was shown in Fig.3.

By taking advantage of this 'locked-phase' property, we can have situations in which the finite-pressure effect rather suppresses islands which have existed in a vacuum field, if the phase of the vacuum field island is opposite to that of the pressure-induced ones. In this section, we directly confirm the existence of such a process in equilibrium calculations.

A vacuum field is shown in Fig.5 (a), where a chain of magnetic islands is formed on the $\iota = 5/6$ rational surface existing in the region of closed surfaces by a specific control of external currents. Shown in Fig.5 (b) is the corresponding finite-β equilibrium with $\beta_0 = 9.0\%$. It is clearly observed that the 5/6 island chain, which existed in the vacuum field, almost completely disappears, and a nice magnetic surface recovers by the effect of 'Self-healing', though the $\iota = 5/6$ surface still exists in the plasma region. When β_0 is further increased, as is shown in Fig.5 (c) for $\beta_0 = 12.0\%$, the position of the $\iota = 5/6$ surface further moves toward the boundary of the plasma, and the 5/6 island chain appears again. Note, however, that the phase of the reappeared 5/6 island chain is opposite to that of the vacuum one. This behaviour confirms that the phase of the finite-pressure-induced island chain is determined irrespective of the vacuum island, and has quite 'robust' nature.

The corresponding change in the ι profile is plotted in Fig.6 for the three cases of β. Here, the $\iota = 5/6$ surface already exists in the vacuum field, and moves toward the plasma boundary

as β increases, which is the relatively higher shear region. Part of the reduction of the island size with the increase of β, shown in Fig.5, could be attributed to the increase in the shear, since the island size w is given as $w^2 \propto \left|(\frac{d\iota}{dr})^{-1} B^{\rho}_{mn}\right|$, where B^{ρ}_{mn} is the magnitude of resonant field perpendicular to the surface. However, the mere shear effect cannot explain the whole process shown here. Namely, it cannot explain the inversion in the phase of islands as is shown in Fig.5 (c), because the shear only influences the magnitude of the island width in a multiplicative way. The magnitude of the resonant field itself, however, which is the direct cause of the islands, is controlled by the finite-pressure effect.

Thus, the island can be kept thin over an appreciable range of β value by making use of this feature.

An interesting additional question in connection with the elimination of the island, see Fig. 5 (b), concerns the consistency of the equilibrium on the rational magnetic surface 5/6 which exists for vanishing island thickness. Here, the so-called Hamada condition [1] that $\int dl/B$ be constant on a rational surface has to hold for a true equilibrium. Evidence is presented that this is indeed so with very good numerical accuracy. With the help of the interface to the VMEC and JMC codes [13], the Jacobian $\sqrt{g}$ in magnetic coordinates (s, θ, ϕ) can easily be obtained and be used to analyze Hamada's condition because of $dl/B \propto \sqrt{g}\, d\phi$. Figure 7 shows that $\sqrt{g}_{6,1}$ (Fourier index notation referring to one period of the equilibrium is used here) is approximately vanishing to very high accuracy so that the Hamada condition is satisfied with this accuracy.

Analogous analysis of the neighbouring equilibria of Fig. 5 shows that in both of these $|\sqrt{g}_{6,1}|$ is significantly larger and of opposite sign in these two cases. The correlation with the island phases appears plausible and suggests that the islated neighboring equilibria are related to a change of sign of a resonant perturbation field so that both its components – parallel to $\vec{B}$ and perpendicular to it – change sign.

IV. DISCUSSION AND SUMMARY

One characteristic of the Helias configuration, which is adopted for the W7-X device, is that it is a low-shear configuration. Therefore, one of the critical issues in obtaining a high-β plasma is imposed by formation of magnetic islands induced in finite-β equilibria. In this paper, a favorable property of the Helias configuration is confirmed that even if a dangerous rational surface exists in the plasma region of Helias, it is not so serious as to destroy the whole plasma, and an equilibrium with reasonably clear surfaces can be obtained up to as

high as $\beta_0 = 15\%$. This result may be attributed to the reduction of the Pfirsch-Schlüter current which is an inherent characteristic of this type of configuration.

Furthermore, a notable property of islands induced due to the finite-pressure effect is found; that is, 'self-healing' of islands as β increases. This feature originates from the property that the finite-pressure-induced islands always have the same phase independent of β. This 'locked-phase' property was discovered here for the first time.

The existence of such a property in the phase of induced islands indicates that finite-pressure-induced islands are governed by resonant magnetic fields generated by 'global' effects of the plasma current density. Namely, the total effect of the plasma current integrated over the whole plasma volume determines the amplitude of the resonant component of the magnetic fields produced on each rational surface. The field generated by such global effects appears to have a specific simple global spatial structure, which results in the 'locked-phase' property of the finite-pressure-induced islands.

Another explanation[14] for the occurence of the 'self-healing' of islands may be possible by extending the analyses of the 'local' effects of plasma currents derived by Cary-Kotschenreuther[4] and Hegna-Bhattacharjee[5]. The physical mechanism of the 'local' effects is completely different from the 'global' effects stated above; those 'local' analyses are irrelevant from the phase property of islands. However, the prediction of those analyses, when extended, does not contradict, at least, with the first stage of the 'self-healing' where the island shrinks as β increases; the configuration has the magnetic well and the D_R (the criteria for the local resistive interchange mode) is stable. (We should note that the second stage, where the island reappears as β increases, is solely explained by the existence of the 'global' effects.) A detailed comparison between the 'local' and 'global' effects will be given in the near future.

The existence of the property of 'self-healing' suggests a possibility to obtain an optimal structure of the internal surfaces at finite β, by properly selecting the 5/6, 5/5, and 5/4 island structures in the vacuum field.

We observe the phenomenon of self-healing of islands not only in Helias but also in $l = 2$ heliotron/torsatron equilibria, although the sizes of induced islands are much smaller than the Helias case. The details will be also reported in the near future.

ACKNOWLEDGMENTS

One of the authors (T.H.) thanks Dr. A.Bhattacharjee for stimulating discussions.

APPENDIX: NUMERICAL GEOMETRY

For the Helias configuration, the shape of the magnetic surfaces changes significantly from cross-section to cross-section in the real space; it is bean-shaped (vertically elongated) at $\phi = 0$ and is triangular (horizontally elongated) at $\phi = \frac{\pi}{M}$, M being the number of periods. Moreover, the magnetic axis is not located on a plane, but has a helical structure. In order that the magnetic surfaces of Helias be covered by the grid box properly, we have slightly modified the geometry of the HINT code[6] as follows. The direction of the grid box rotates as $\theta = \frac{M}{2}\phi$, where θ is the poloidal angle, while it rotated as $\theta = M\phi$ for the calculations of $l = 2$ heliotron/torsatron configurations. On the other hand, the central position of the grid box rotates as $\theta = M\phi$ with the minor radius δ_c, which roughly follows the helical position of the magnetic axis of Helias. Consequently, the relation between the coordinate of the grid points (u^1, u^2, u^3) and the Cartesian coordinate (x, y, z) is given as follows;

$$x = (R_0 + u^1_* \cos hu^3 + u^2_* \sin hu^3)\cos u^3 \tag{1}$$

$$y = -(R_0 + u^1_* \cos hu^3 + u^2_* \sin hu^3)\sin u^3 \tag{2}$$

$$z = -u^1_* \sin hu^3 + u^2_* \cos hu^3 \tag{3}$$

with

$$u^1_* = u^1 + \delta_c \cos hu^3 \tag{4}$$

$$u^2_* = u^2 - \delta_c \sin hu^3 \tag{5}$$

and

$$u^3 = -\phi, \tag{6}$$

where $h = \frac{M}{2}$, and R_0 is basic major radius (constant). Correspondingly, the covariant components of the metric g_{ij}, which is defined as

$$g_{ij} = \frac{\partial \boldsymbol{r}}{\partial u^i} \cdot \frac{\partial \boldsymbol{r}}{\partial u^j}$$

are given as

$$g_{11} = 1,\ g_{12} = 0,\ g_{22} = 1 \tag{7}$$

$$g_{13} = hu^2_* - h\delta_c \sin hu^3 \tag{8}$$

$$g_{23} = -hu^1_* - h\delta_c \cos hu^3 \tag{9}$$

$$g_{33} = (R_0 + u^1_* \cos hu^3 + u^2_* \sin hu^3)^2 + h^2(u^1_*)^2 + h^2(u^2_*)^2 + h^2\delta_c^2 + 2h^2\delta_c(u^1_* \cos hu^3 - u^2_* \sin hu^3). \tag{10}$$

The Jacobian J is described as

$$J = \sqrt{det(g_{ij})} = R_0 + u^1_* \cos hu^3 + u^2_* \sin hu^3. \tag{11}$$

Other features of the code are the same as before. Namely, the equilibrium calculation is made on the Eulerian coordinate (u^1, u^2, u^3) by making use of an initial value method, where a difference scheme with 4th order accuracy in both time and space is utilized. Free boundary conditions are used, for which the shape and the location of the boundary magnetic surface can change. In some cases the boundary is ergodized, as β increases. A net-current free equilibrium is obtained. The calculation is made for half a field period of the torus, keeping, what is called, the stellarator symmetry as the boundary condition in the toroidal direction.

REFERENCES

[1] S. Hamada, Nucl. Fusion **2**, 23 (1962).

[2] H. Grad, Phys. Fluids **10**, 137 (1967).

[3] A.H. Reiman and A.H. Boozer, Phys. Fluids **27**, 2446 (1984).

[4] J.R. Cary and M. Kotschenreuther, Phys. Fluids **28**, 1392 (1985).

[5] C.C. Hegna, A. Bhattacharjee, Phys. Fluids B **1**, 392 (1989); C.C. Hegna, A. Bhattacharjee, Y. Nakamura, and M. Wakatani, Phys. Fluids B **3**, 2285 (1991)

[6] K. Harafuji, T. Hayashi, and T. Sato, J. Comput. Phys. **81**, 169 (1989).

[7] T. Hayashi, T. Sato, and A. Takei, Phys. Fluids B **2**, 329 (1990).

[8] T. Hayashi, A. Takei, N. Ohyabu, and T. Sato, Nucl. Fusion **31**, 1767 (1991).

[9] T. Hayashi, A. Takei, and T. Sato, Phys. Fluids B **4**, 1539 (1992).

[10] J. Nührenberg and R. Zille, Phys. Letters **114**, 129 (1986).

[11] G. Grieger, C.D. Beidler, H. Maassberg, E. Harmeyer, F. Herrnegger, J. Junker, J. Kisslinger, W. Lotz, P. Merkel, J. Nührenberg, F. Rau, J. Sapper, A. Schlüter, F. Sardei, and H. Wobig, in *Plasma Physics and Controlled Fusion Research* (International Atomic Energy Agency, Vienna, 1991), Vol.3, p.525.

[12] T. Hayashi, U. Schwenn, and E. Strumberger, Jpn. J. Appl. Phys. **31**, 2580 (1992).

[13] T. Hayashi, U. Schwenn, P. Merkel, IPP 2/313, 48 (1991).

[14] A. Bhattacharjee, (private communication, 1993).

FIGURE CAPTIONS

Fig.1 Poincaré plots of magnetic field lines for a Helias vacuum field at two poloidal cross sections, $\phi = 0$ (right,'bean-shaped') and $\phi = \frac{\pi}{5}$ (left,'triangular'). The $\frac{5}{5}$ vacuum island chain is observed near the boundary. The outer rectangles indicate the location of the grid box.

Fig.2 Radial profiles of the rotational transform ι and the magnetic well W for (a) vacuum field, and (b) finite-β equilibrium field ($\beta_0 = 7.2\%$), of Helias. The $\frac{5}{6}$ rational surface is avoided in the vacuum field, but comes into the plasma region in the finite-β field.

Fig.3 Poincaré plots of magnetic field lines for a finite-β equilibrium ($\beta_0 = 7.2\%$) of Helias at two poloidal cross sections, $\phi = 0$ (right) and $\phi = \frac{\pi}{5}$ (left). The $\frac{5}{6}$ island chain occurs and resides at about half the plasma radius in a position of vanishing shear, but is not so serious as to destroy the whole plasma. The $\frac{5}{5}$ island chain lies in the boundary ergodic region, but the positions do not vary significantly compared with the vacuum field (Fig.1).

Fig.4 Contour of plasma pressure p for the same finite-β equilibrium as Fig.3. Corresponding to the formation of the $\frac{5}{6}$ magnetic island, island structure is formed also in the pressure profile.

Fig.5 Poincaré plots of magnetic field lines to show the process of 'self-healing' of magnetic islands for Helias. (a) A vacuum field, where a chain of $\frac{5}{6}$ island is formed externally. (b) The island gradually shrinks as β increases, and finally disappears ($\beta_0 = 9\%$). (c) When β is further increased, the island chain appears again, but with the inverted phase from the vacuum one ($\beta_0 = 12\%$).

Fig.6 Radial profile of the rotational transform for three cases of β, corresponding to Fig.5, where the 'self-healing' of magnetic islands occurs.

Fig.7 Various Fourier coefficients $\sqrt{g}_{m,n}$, normalized to $\sqrt{g}_{0,0}$ as functions of a normalized radius (square root of normalized toroidal flux); m, n refer to the poloidal and toroidal magnetic coordinate dependencies in an equilibrium notation in which $n = 1$ is related to the fundamental period within one of the five equilibrium periods. The position of the 5/6 (in this equilibrium notation 1/6) resonance is also indicated.

Helias

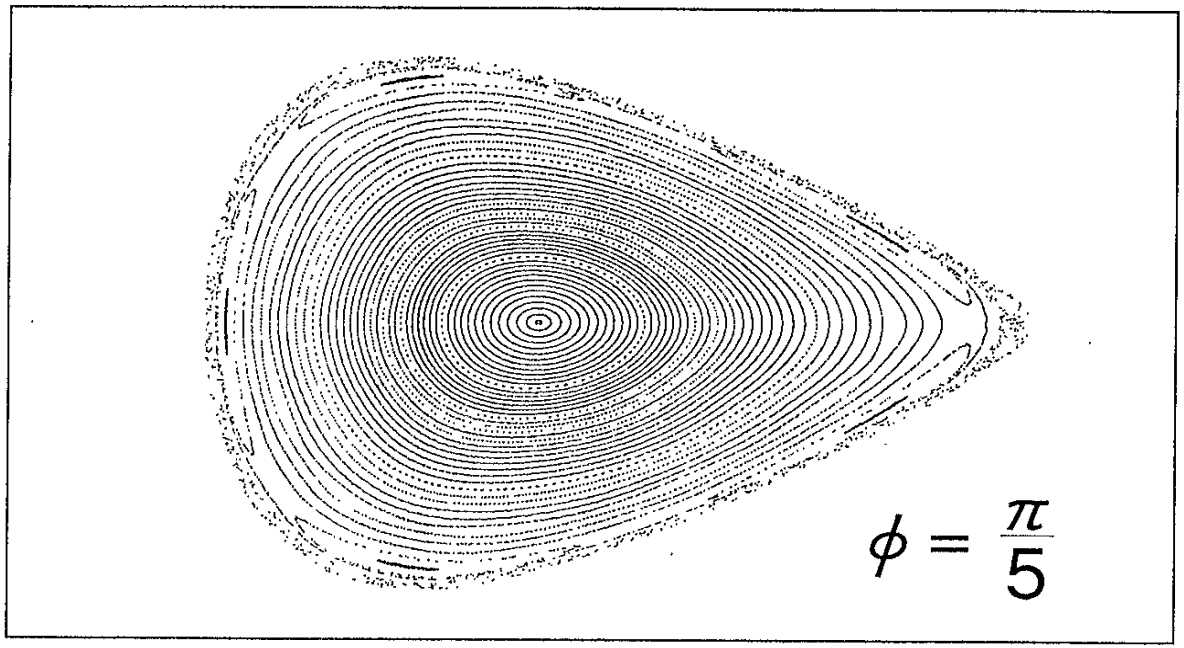

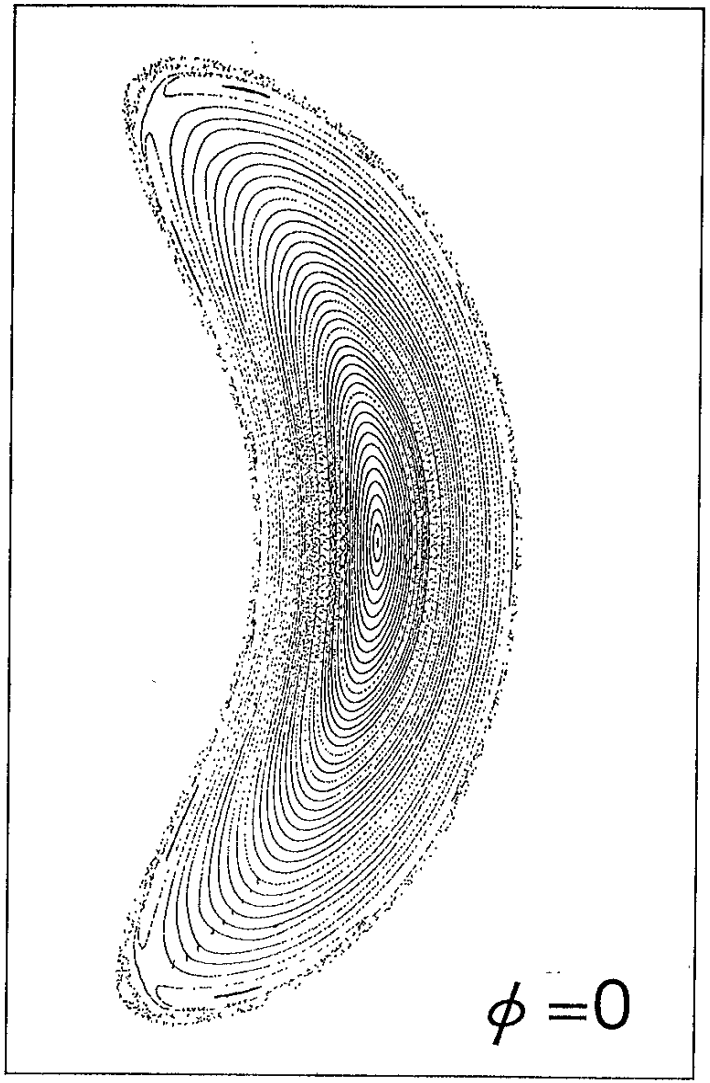

Vacuum Field

Fig.1

(a) Vacuum Field

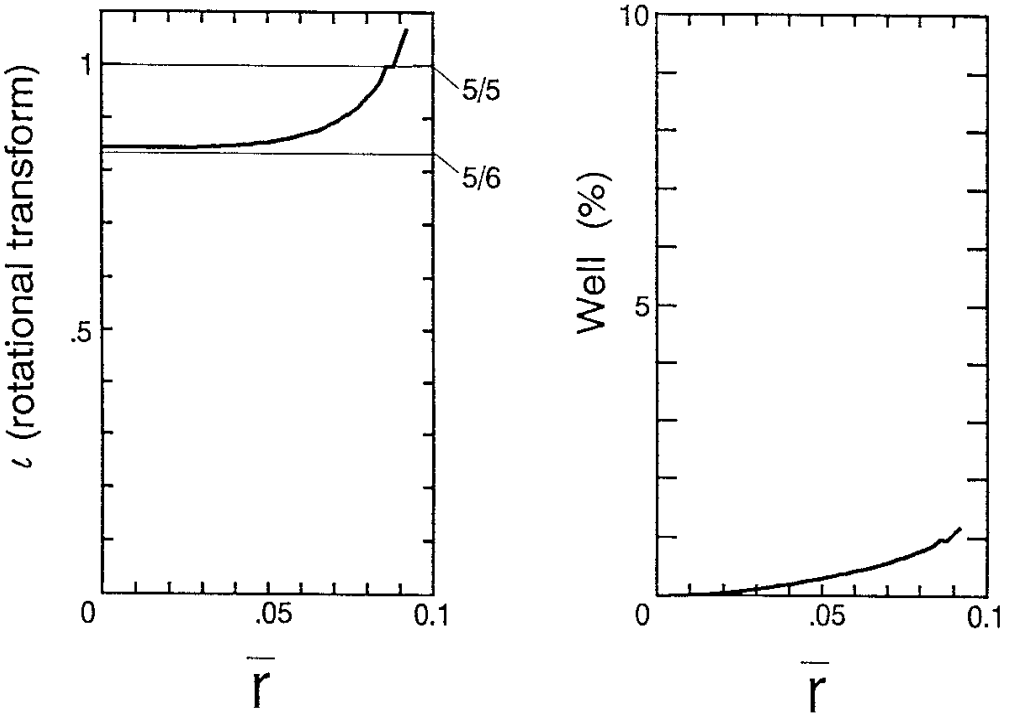

(b) $\beta_0 = 7.2\%$

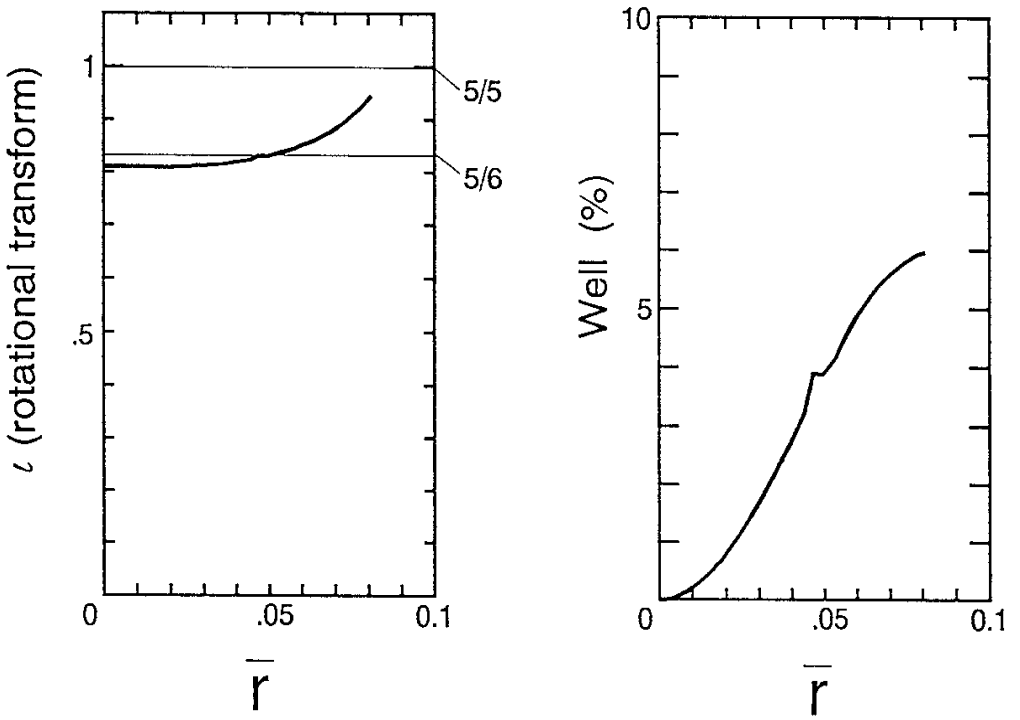

Fig.2

Helias

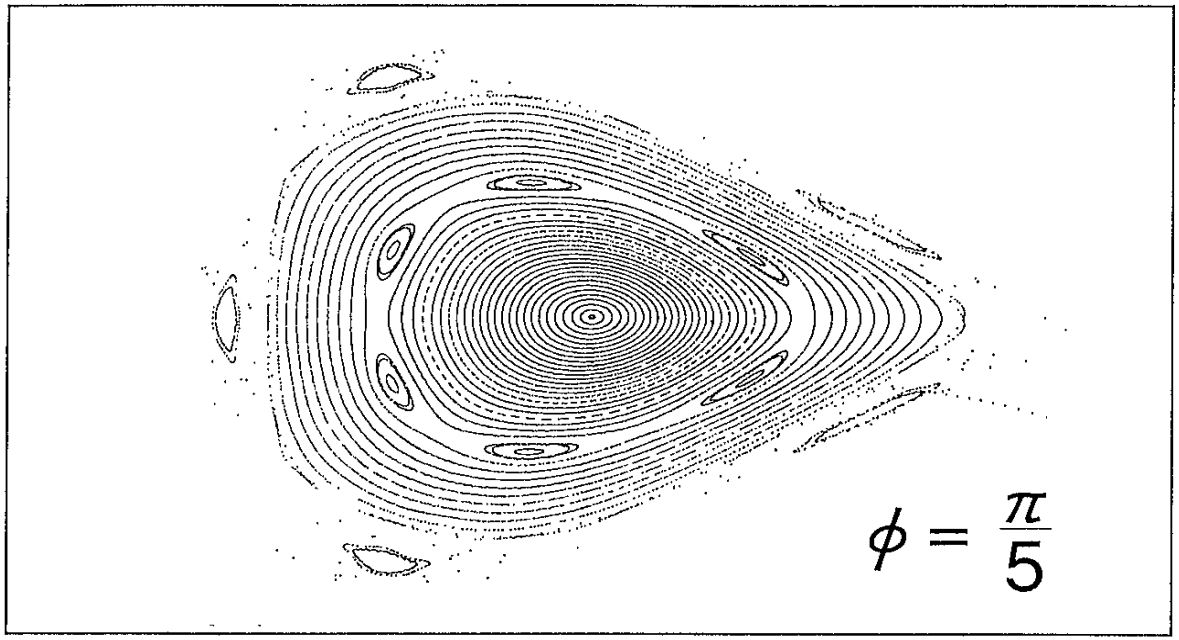

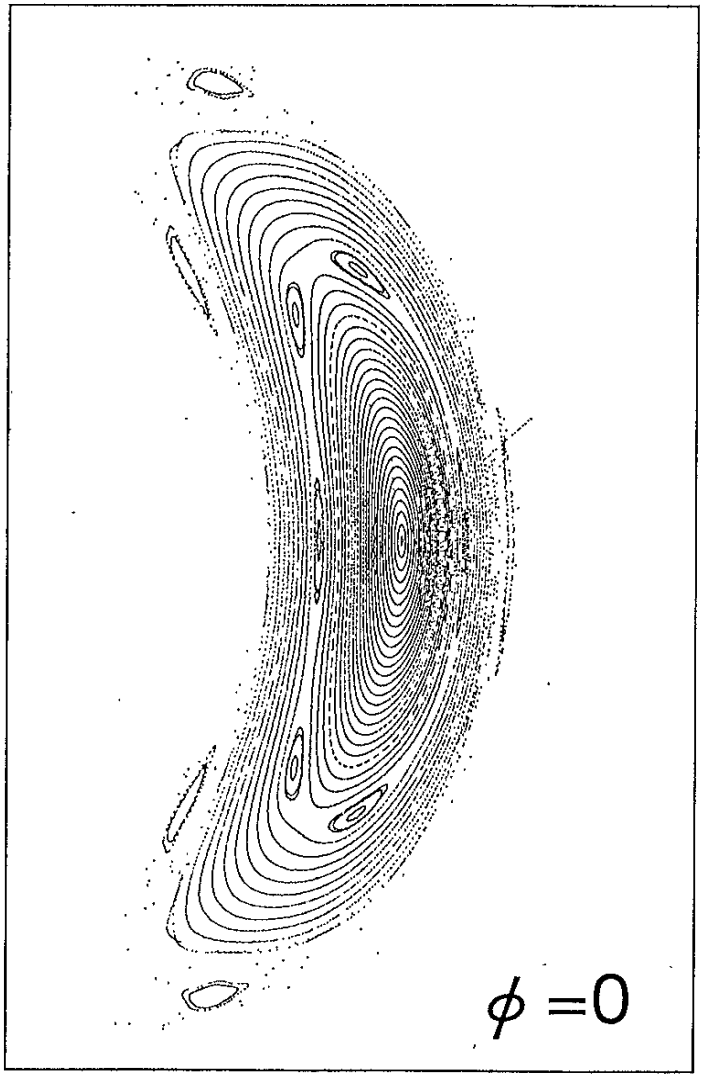

$\beta_0 = 7.2\%$

Fig.3

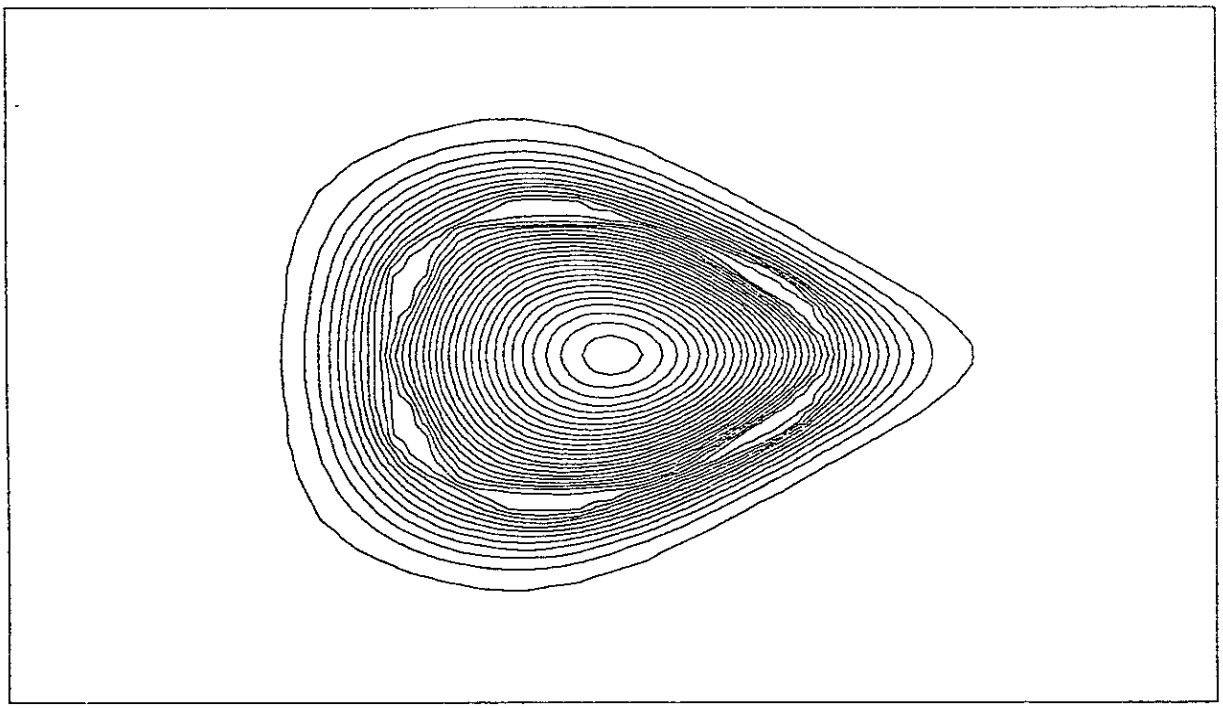

Fig.4

(a) Vacuum Field

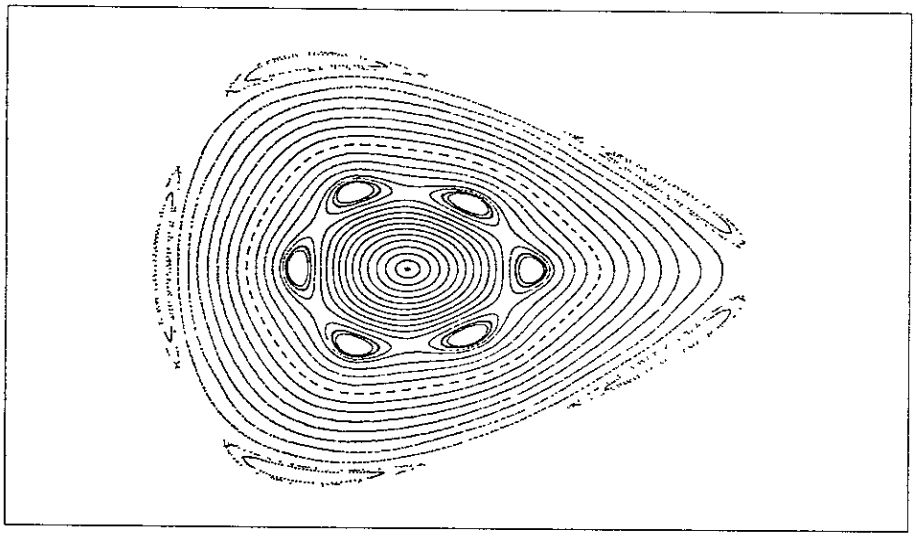

(b) $\beta_0 = 9\%$

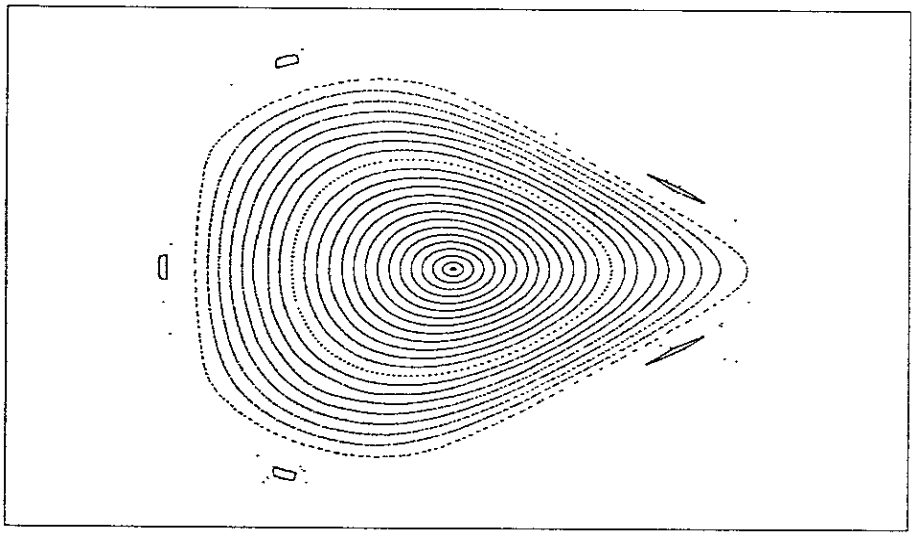

(c) $\beta_0 = 12\%$

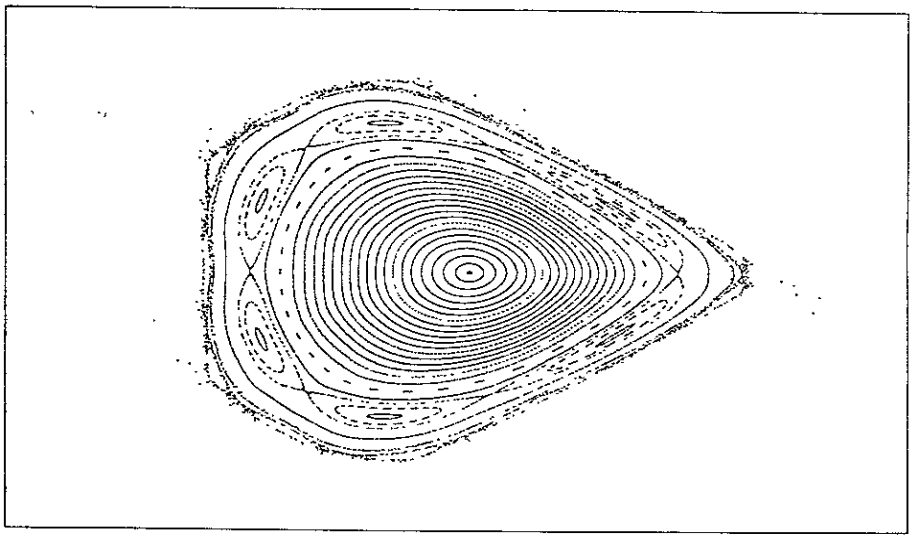

Fig.5

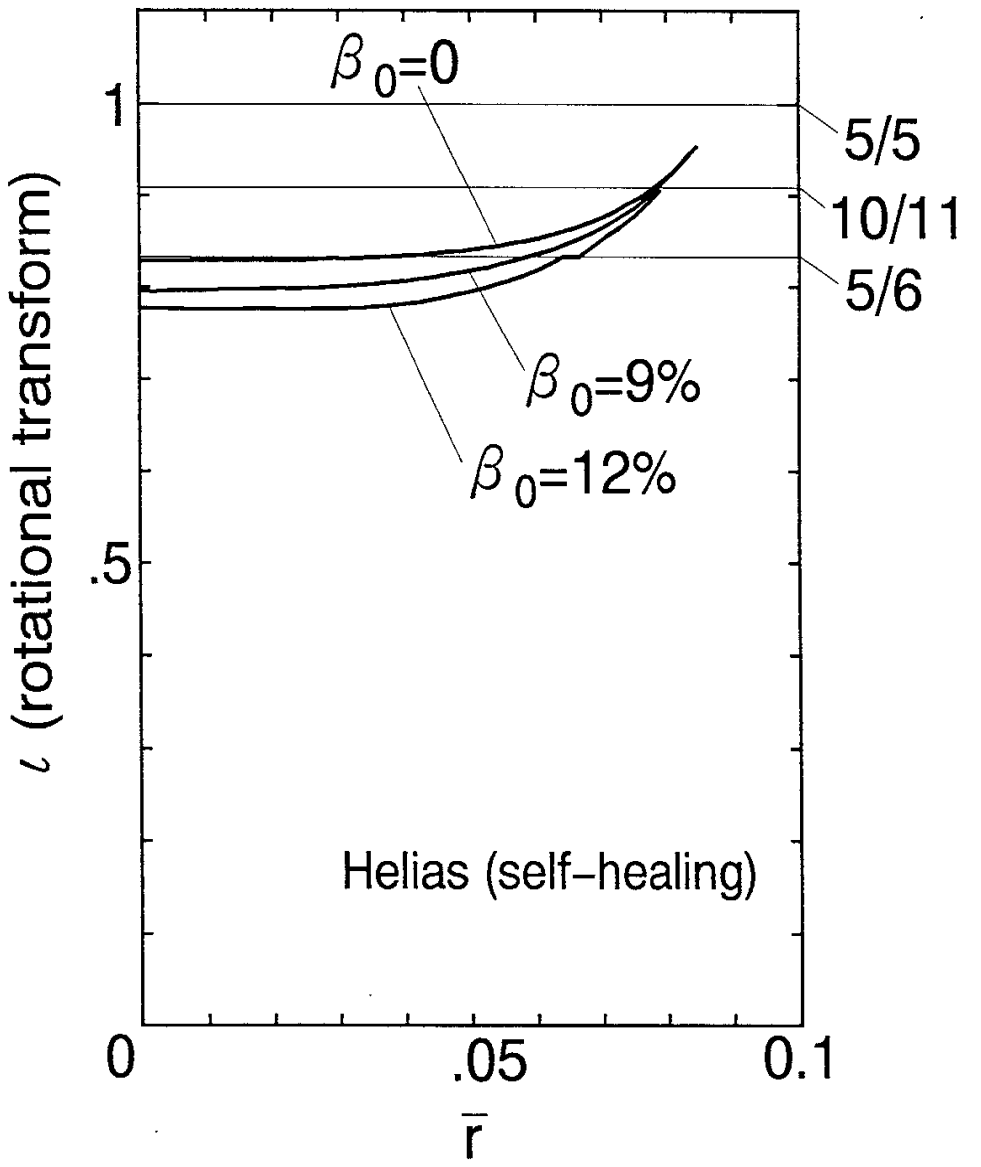
β_0=0
β_0=9%
β_0=12%
5/5
10/11
5/6
1
.5
0
.05
0.1
$\bar{r}$
ι (rotational transform)
Helias (self-healing)

Fig.6

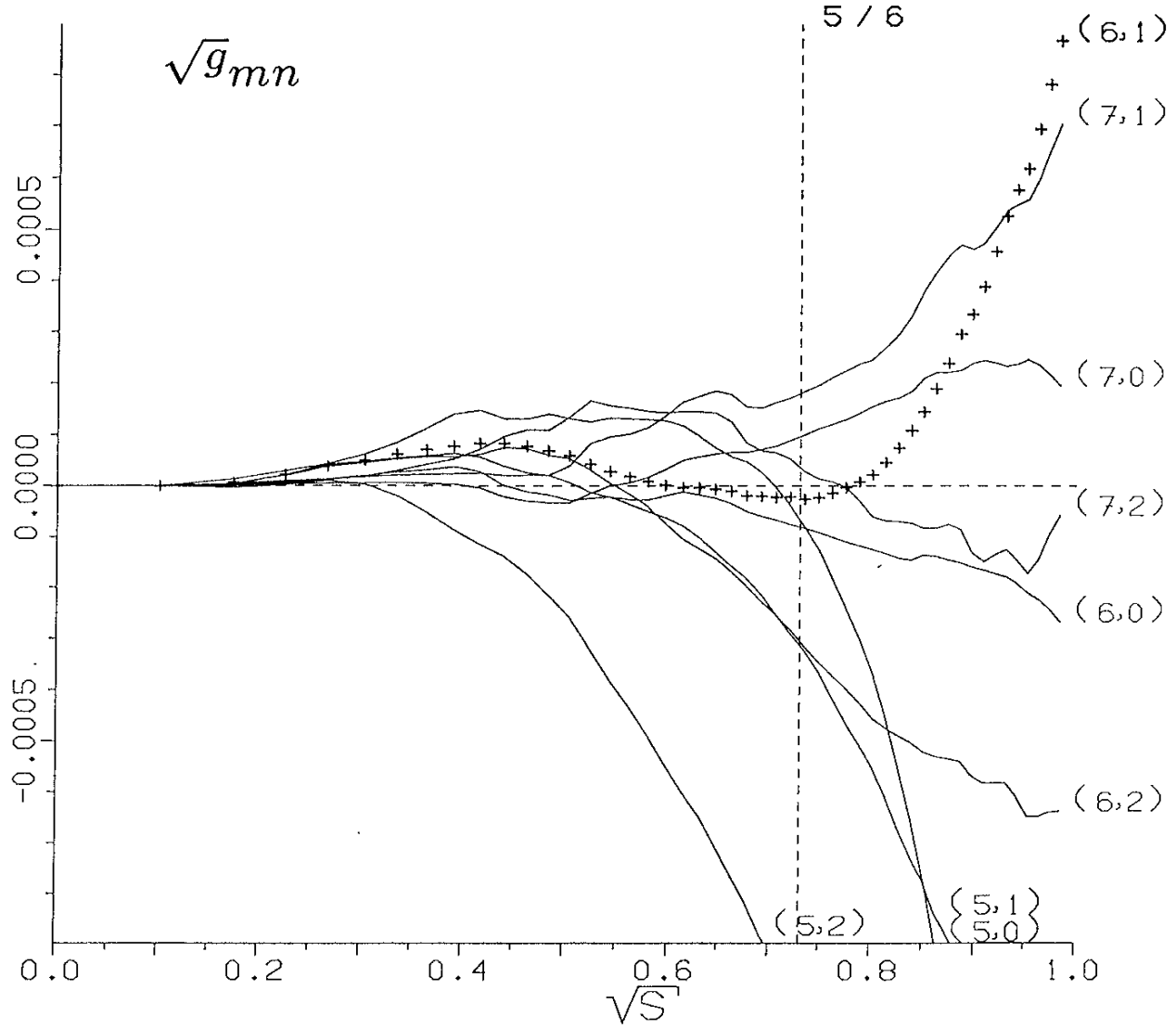
$\sqrt{g_{mn}}$
5 / 6
(6,1)
(7,1)
(7,0)
(7,2)
(6,0)
(6,2)
(5,2)
(5,1)
(5,0)
0.0005
0.0000
-0.0005
0.0
0.2
0.4
0.6
0.8
1.0
$\sqrt{S}$

Fig.7

Recent Issues of NIFS Series

NIFS-220 T. Watari, R. Kumazawa, T. Mutoh, T. Seki, K. Nishimura and F. Shimpo, *Applications of Non-resonant RF Forces to Improvement of Tokamak Reactor Performances Part I: Application of Ponderomotive Force* ; May 1993

NIFS-221 S.-I. Itoh, K. Itoh, and A. Fukuyama, *ELMy-H mode as Limit Cycle and Transient Responses of H-modes in Tokamaks* ; May 1993

NIFS-222 H. Hojo, M. Inutake, M. Ichimura, R. Katsumata and T. Watanabe, *Interchange Stability Criteria for Anisotropic Central-Cell Plasmas in the Tandem Mirror GAMMA 10 ;* May 1993

NIFS-223 K. Itoh, S.-I. Itoh, M. Yagi, A. Fukuyama and M. Azumi, *Theory of Pseudo-Classical Confinement and Transmutation to L-Mode;* May 1993

NIFS-224 M. Tanaka, *HIDENEK: An Implicit Particle Simulation of Kinetic-MHD Phenomena in Three-Dimensional Plasmas;* May 1993

NIFS-225 H. Hojo and T. Hatori, *Bounce Resonance Heating and Transport in a Magnetic Mirror;* May 1993

NIFS-226 S.-I. Iton, K. Itoh, A. Fukuyama, M. Yagi, *Theory of Anomalous Transport in H-Mode Plasmas;* May 1993

NIFS-227 T. Yamagishi, *Anomalous Cross Field Flux in CHS ;* May 1993

NIFS-228 Y. Ohkouchi, S. Sasaki, S. Takamura, T. Kato, *Effective Emission and Ionization Rate Coefficients of Atomic Carbons in Plasmas;* June 1993

NIFS-229 K. Itoh, M. Yagi, A. Fukuyama, S.-I. Itoh and M. Azumi, *Comment on 'A Mean Field Ohm's Law for Collisionless Plasmas;* June 1993

NIFS-230 H. Idei, K. Ida, H. Sanuki, H. Yamada, H. Iguchi, S. Kubo, R. Akiyama, H. Arimoto, M. Fujiwara, M. Hosokawa, K. Matsuoka, S. Morita, K. Nishimura, K. Ohkubo, S. Okamura, S. Sakakibara, C. Takahashi, Y. Takita, K. Tsumori and I. Yamada, *Transition of Radial Electric Field by Electron Cyclotron Heating in Stellarator Plasmas;* June 1993

NIFS-231 H.J. Gardner and K. Ichiguchi, *Free-Boundary Equilibrium Studies for the Large Helical Device,* June 1993

NIFS-232 K. Itoh, S.-I. Itoh, A. Fukuyama, H. Sanuki and M. Yagi, *Confinement Improvement in H-Mode-Like Plasmas in Helical Systems,* June 1993

NIFS-233 R. Horiuchi and T. Sato, *Collisionless Driven Magnetic Reconnection,* June 1993

NIFS-234 K. Itoh, S.-I. Itoh, A. Fukuyama, M. Yagi and M. *Azumi, Prandtl Number of Toroidal Plasmas;* June 1993

NIFS-235 S. Kawata, S. Kato and S. Kiyokawa , *Screening Constants for Plasma;* June 1993

NIFS-236 A. Fujisawa and Y. Hamada, *Theoretical Study of Cylindrical Energy Analyzers for MeV Range Heavy Ion Beam Probes;* July 1993

NIFS-237 N. Ohyabu, A. Sagara, T. Ono, T. Kawamura and O. Motojima, *Carbon Sheet Pumping;* July 1993

NIFS-238 K. Watanabe, T. Sato and Y. Nakayama, *Q-profile Flattening due to Nonlinear Development of Resistive Kink Mode and Ensuing Fast Crash in Sawtooth Oscillations;* July 1993

NIFS-239 N. Ohyabu, T. Watanabe, Hantao Ji, H. Akao, T. Ono, T. Kawamura, K. Yamazaki, K. Akaishi, N. Inoue, A. Komori, Y. Kubota, N. Noda, A. Sagara, H. Suzuki, O. Motojima, M. Fujiwara, A. Iiyoshi, *LHD Helical Divertor;* July 1993

NIFS-240 Y. Miura, F. Okano, N. Suzuki, M. Mori, K. Hoshino, H. Maeda, T. Takizuka, JFT-2M Group, K. Itoh and S.-I. Itoh, *Ion Heat Pulse after Sawtooth Crash in the JFT-2M Tokamak;* Aug. 1993

NIFS-241 K. Ida, Y.Miura, T. Matsuda, K. Itoh and JFT-2M Group, *Observation of non Diffusive Term of Toroidal Momentum Transport in the JFT-2M Tokamak;* Aug. 1993

NIFS-242 O.J.W.F. Kardaun, S.-I. Itoh, K. Itoh and J.W.P.F. Kardaun, *Discriminant Analysis to Predict the Occurrence of ELMS in H-Mode Discharges;* Aug. 1993

NIFS-243 K. Itoh, S.-I. Itoh, A. Fukuyama, *Modelling of Transport Phenomena;* Sep. 1993

NIFS-244 J. Todoroki, *Averaged Resistive MHD Equations;* Sep. 1993

NIFS-245 M. Tanaka, *The Origin of Collisionless Dissipation in Magnetic Reconnection;* Sep. 1993

NIFS-246 M. Yagi, K. Itoh, S.-I. Itoh, A. Fukuyama and M. Azumi, *Current Diffusive Ballooning Mode in Seecond Stability Region of*

Tokamaks; Sep. 1993

NIFS-247 T. Yamagishi,
Trapped Electron Instabilities due to Electron Temperature Gradient and Anomalous Transport; Oct. 1993

NIFS-248 Y. Kondoh,
Attractors of Dissipative Structure in Three Disspative Fluids; Oct. 1993

NIFS-249 S. Murakami, M. Okamoto, N. Nakajima, M. Ohnishi, H. Okada,
Monte Carlo Simulation Study of the ICRF Minority Heating in the Large Helical Device; Oct. 1993

NIFS-250 A. Iiyoshi, H. Momota, O. Motojima, M. Okamoto, S. Sudo, Y. Tomita, S. Yamaguchi, M. Ohnishi, M. Onozuka, C. Uenosono,
Innovative Energy Production in Fusion Reactors; Oct. 1993

NIFS-251 H. Momota, O. Motojima, M. Okamoto, S. Sudo, Y. Tomita, S. Yamaguchi, A. Iiyoshi, M. Onozuka, M. Ohnishi, C. Uenosono,
Characteristics of D-^{3}He Fueled FRC Reactor: ARTEMIS-L,
Nov. 1993

NIFS-252 Y. Tomita, L.Y. Shu, H. Momota,
Direct Energy Conversion System for D-^{3}He Fusion, Nov. 1993

NIFS-253 S. Sudo, Y. Tomita, S. Yamaguchi, A. Iiyoshi, H. Momota, O. Motojima, M. Okamoto, M. Ohnishi, M. Onozuka, C. Uenosono,
Hydrogen Production in Fusion Reactors, Nov. 1993

NIFS-254 S. Yamaguchi, A. Iiyoshi, O. Motojima, M. Okamoto, S. Sudo, M. Ohnishi, M. Onozuka, C. Uenosono,
Direct Energy Conversion of Radiation Energy in Fusion Reactor,
Nov. 1993

NIFS-255 S. Sudo, M. Kanno, H. Kaneko, S. Saka, T. Shirai, T. Baba,
Proposed High Speed Pellet Injection System "HIPEL" for Large Helical Device
Nov. 1993

NIFS-256 S. Yamada, H. Chikaraishi, S. Tanahashi, T. Mito, K. Takahata, N. Yanagi, M. Sakamoto, A. Nishimura, O. Motojima, J. Yamamoto, Y. Yonenaga, R. Watanabe,
Improvement of a High Current DC Power Supply System for Testing the Large Scaled Superconducting Cables and Magnets; Nov. 1993

NIFS-257 S. Sasaki, Y. Uesugi, S. Takamura, H. Sanuki, K. Kadota,
Temporal Behavior of the Electron Density Profile During Limiter Biasing in the HYBTOK-II Tokamak; Nov. 1993

NIFS-258 K. Yamazaki, H. Kaneko, S. Yamaguchi, K.Y. Watanabe, Y.Taniguchi, O.Motojima, LHD Group,
Design of Central Control System for Large Helical Device (LHD); Nov. 1993

NIFS-259 K. Yamazaki, H. Kaneko, S. Yamaguchi, K.Y. Watanabe, Y.Taniguchi, O.Motojima, LHD Group,
Design of Central Control System for Large Helical Device (LHD); Nov. 1993

NIFS-260 B.V.Kuteev,
Pellet Ablation in Large Helical Device; Nov. 1993

NIFS-261 K. Yamazaki,
Proposal of "MODULAR HELIOTRON': Advanced Modular Helical System Compatible with Closed Helical Divertor; Nov. 1993

NIFS-262 V.D.Pustovitov,
Some Theoretical Problems of Magnetic Diagnostics in Tokamaks and Stellarators; Dec. 1993

NIFS-263 A. Fujisawa, H. Iguchi, Y. Hamada
A Study of Non-Ideal Focus Properties of 30° Parallel Plate Energy Analyzers; Dec. 1993

NIFS-264 K. Masai,
Nonequilibria in Thermal Emission from Supernova Remnants; Dec. 1993

NIFS-265 K. Masai, K. Nomoto,
X-Ray Enhancement of SN 1987A Due to Interaction with its Ring-like Nebula; Dec. 1993

NIFS-266 J. Uramoto
A Research of Possibility for Negative Muon Production by a Low Energy Electron Beam Accompanying Ion Beam; Dec. 1993

NIFS-267 H. Iguchi, K. Ida, H. Yamada, K. Itoh, S.-I. Itoh, K. Matsuoka, S. Okamura, H. Sanuki, I. Yamada, H. Takenaga, K. Uchino, K. Muraoka,
The Effect of Magnetic Field Configuration on Particle Pinch Velocity in Compact Helical System (CHS); Jan. 1993

NIFS-268 T. Shikama, C. Namba, M. Kosuda, Y. Maeda,
Development of High Time-Resolution Laser Flash Equipment for Thermal Diffusivity Measurements Usting Miniature-Size Specimens; Jan. 1994